Supporting Information

CRISPR-Cas12a Amplified RNase Activity Sensor Powered by Gold Nanoparticle–Barcode DNA Multipliers

Sathishkumar Munusamy, Rana Jahani, Jun Chen, Shuo Zhou, Juanhua Kong, Haiyan Zheng*, and Xiyun Guan*

Author affiliation:

Department of Chemistry, University of Missouri, Columbia, MO 65211, USA

*Corresponding Author E-mails: haiyanzheng1111@gmail.com and xgpc2@missouri.edu

Table of Contents:

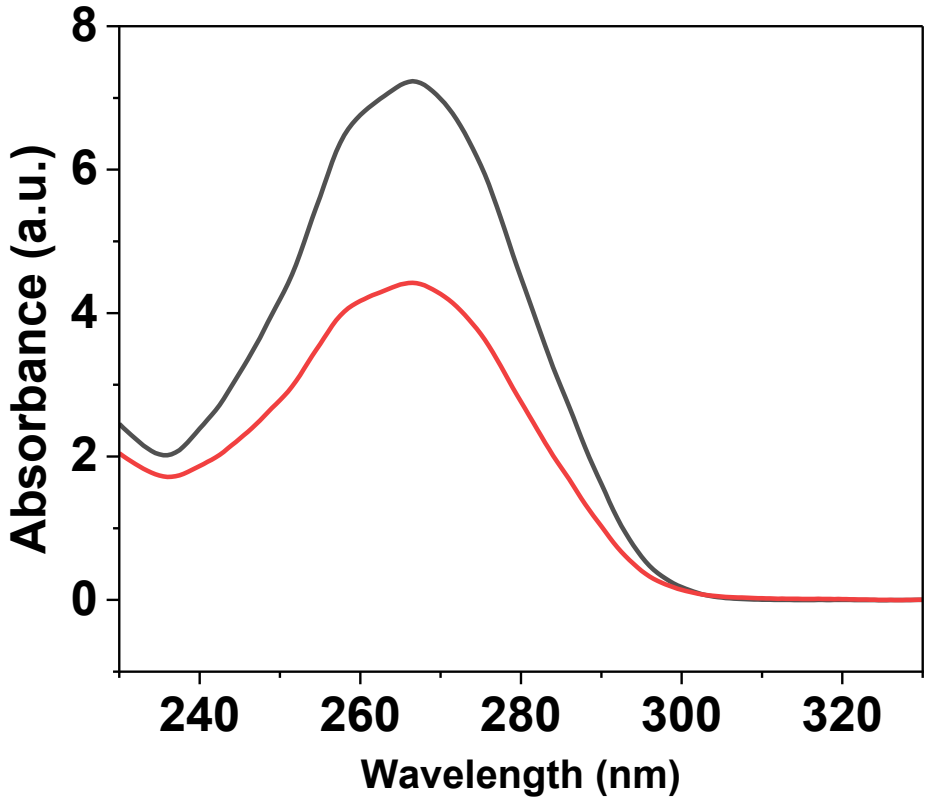

Figure S1. Quantification of oligonucleotide loading on AuNPs by UV–vis. The black absorption spectrum referred to the free oligonucleotide solution before AuNPs modification, while the red one corresponded to the supernatant collected after centrifugation of the AuNP–oligonucleotide conjugates. The amount of oligonucleotide immobilized on the AuNP surface was determined based on the difference in the absorbance between the supernatant and the control.

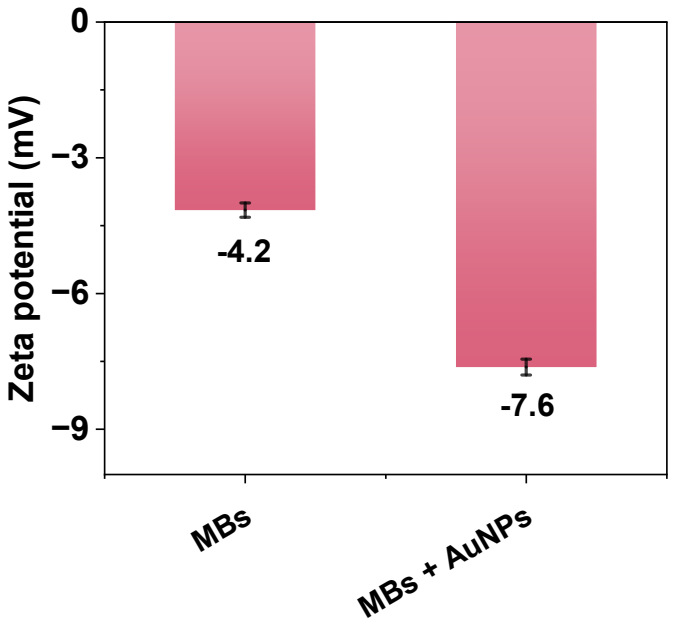

Figure S2. Zeta potential of streptavidin-coated magnetic beads (MBs) before and after conjugation with nucleic acid-functionalized AuNPs, confirming successful SB-MAC assembly via biotin–streptavidin interaction.

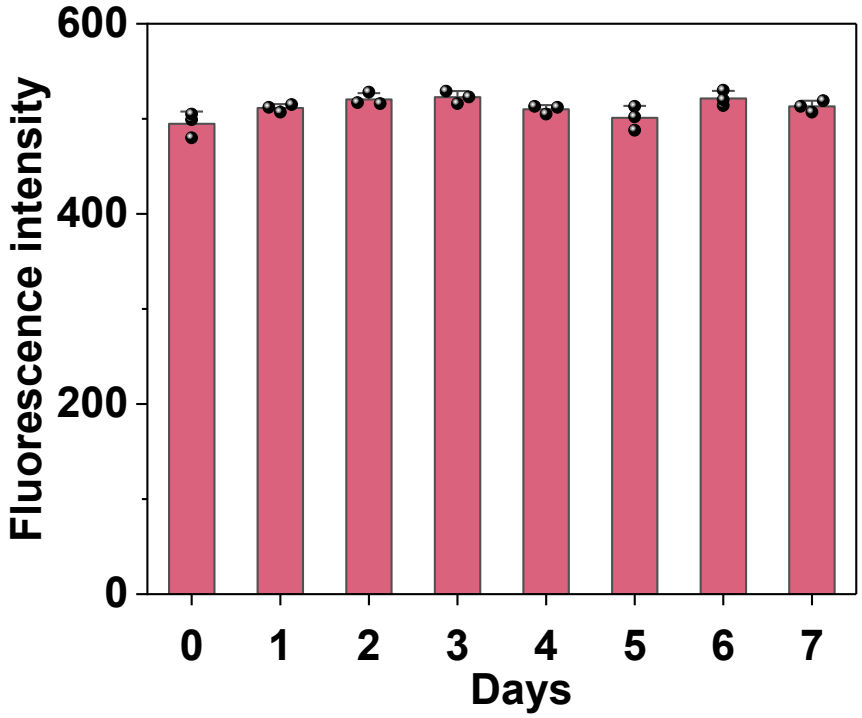

Figure S3. Stability study of the prepared SB-MAC assemblies, indicating no detectable dissociation of the functionalized AuNPs or barcode DNA from the assemblies. In Fig. S3, the supernatants of freshly prepared SB-MAC assemblies and those stored at 4 °C for up to 7 days were analyzed using the CRISPR system, which consisted of Cas12a, crRNA (sequence: rUrArArUrUrUrCrUrArCrUrArArGrUrGrUrArGrArUrArArArArArArArArArArArArArArArArA rArArArATATTATT), and dye-labeled reporter DNA (sequence: FAM–TTATT–IABkFQ).

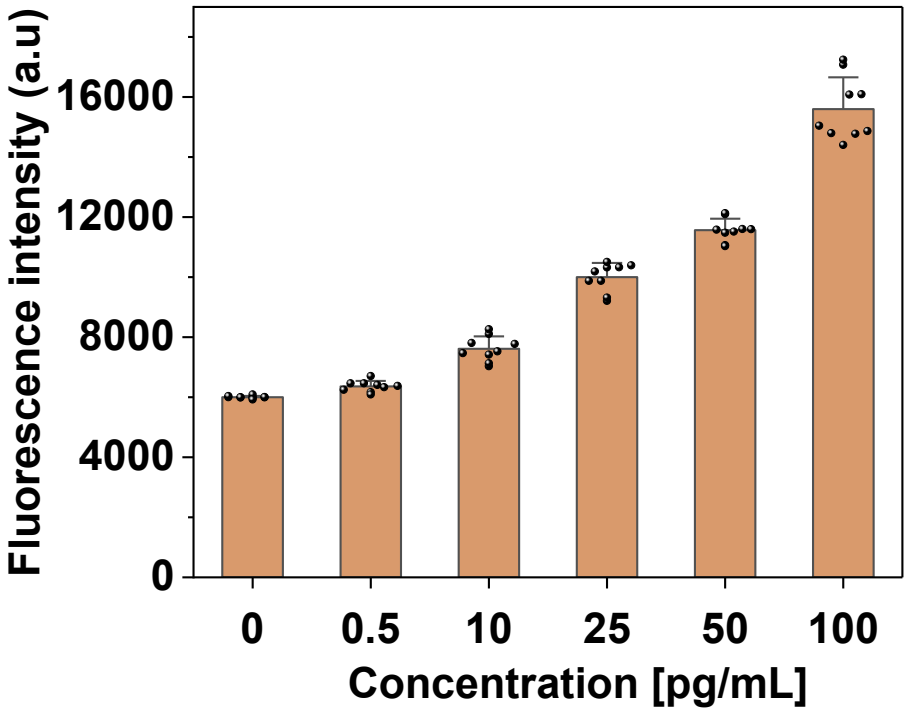

Figure S4. Reproducibility study of the DNA-assisted CRISPR-Cas12a sensing platform for RNase A detection. The error bars indicate the average and standard deviation values derived from results obtained in nine independent experiments (n = 9), encompassing both batch-to-batch and day-to-day variability.

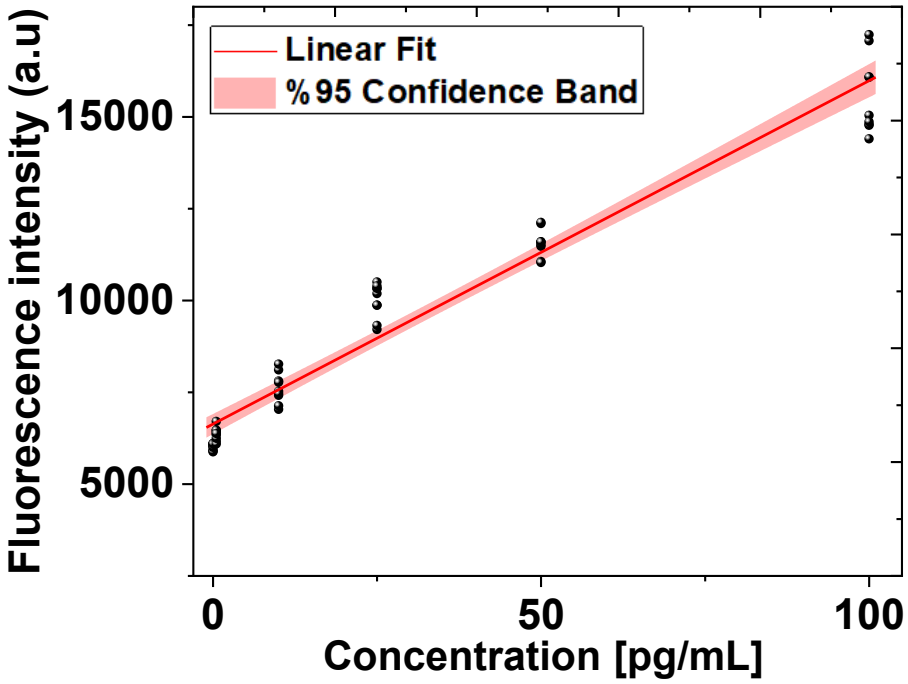

Figure S5. Relationship between fluorescence intensity and RNase A concentration.

Table S1. Performance comparison of the developed RNase activity assay with other reported detection methods

Materials	Methods	LOD (pg/mL)	Ref.
Reduced graphene oxide (rGO)	Fluorescence	50	[1]
A $Ru(bpy)_3^{2+}$-labeled rU-containing chimeric DNA probe	Electrochemiluminescence	0.2	[2]
Au nanoparticles/SnO_2/$ZnIn_2S_4$	Photoelectrochemical / electrochemical	0.2	[3]
Thioflavin T	luminescence	24.7	[4]
rGO–DNAzyme	Fluorescence	89	[5]
Tetrahedral DNA nanoprobe	Fluorescence	90	[6]
Fe_3O_4/multi-walled carbon nanotubes/SiO_2-surface	Chemiluminescence	0.32	[7]
Electrode immobilized with a ferrocenyl cytidine-DNA probe	Electrochemical	10	[8]
Styryl dye	Fluorescence	2.87	[9]
Dual functionalized gold nanoparticles	Fluorescence	0.16	The sensor developed in this work

References

[1] C. Tong, C. Zhao, B. Liu, B. Li, Z. Ai, J. Fan, W. Wang, Sensitive detection of RNase A activity and collaborative drug screening based on rGO and fluorescence probe, Anal. Chem. 90 (2018) 2655–2661. https://doi.org/10.1021/acs.analchem.7b04429.

[2] J. Ni, H. Lin, W. Yang, Y. Liao, Q. Wang, F. Luo, L. Guo, B. Qiu, Z. Lin, Homogeneous electrochemiluminescence biosensor for the detection of RNase A activity and its inhibitor, Anal. Chem. 91 (2019) 14751–14756. https://doi.org/10.1021/acs.analchem.9b04194.

[3] Y. Ying, M. Zhou, S. Dai, M. Ma, W. Deng, Y. Tan, Q. Xie, Au nanoparticles/SnO2/ZnIn2S4-based biosensor for photoelectrochemical/electrochemical dual-signal detection of RNase A by combining the enzymolysis of DNA probe and the generation of molybdophosphate precipitate, Sens. Actuators B Chem. 354 (2022) 131251. https://doi.org/10.1016/j.snb.2021.131251.

[4] J. Du, Y. Dong, H. Liu, L. Gong, S. Lu, C. Yang, Y. Li, Thioflavin T as luminescence biosensors for nucleic acid study and RNase A activity detection, Microchem. J. 147 (2019) 842–847. https://doi.org/10.1016/j.microc.2019.04.008.

[5] Y. Qin, Y. Long, T. Zhou, R. Luo, C. Tong, Q. Xie, W. Wang, B. Liu, A rGO–DNAzyme assisted fluorescence method for sensitive RNase A activity assay and natural compound screening, Anal. Methods 13 (2021) 4298–4306. https://doi.org/10.1039/D1AY01053K.

[6] C. Tong, Y. Hu, Q. Xie, T. Zhou, J. Fan, Y. Qin, B. Liu, W. Wang, Sensitive RNase A detection and intracellular imaging using a natural compound-assisted tetrahedral DNA nanoprobe, Chem. Commun. 56 (2020) 3229–3232. https://doi.org/10.1039/D0CC00284D.

[7] H. Duan, L. Li, X. Wang, Y. Wang, J. Li, C. Luo, Biorecognition and highly sensitive determination of Ribonuclease A with chemiluminescence sensor based on Fe3O4/multi-walled carbon nanotubes/SiO2-surface molecular imprinting polymer, RSC Adv. 5 (2015) 18850–18857. https://doi.org/10.1039/C4RA16878J.

[8] S. Sato, S. Takenaka, Electrochemical RNase A detection using an electrode with immobilized ferrocenyl deoxyribooligonucleotide containing cytidine residue, Electroanalysis 25 (2013) 1652–1658. https://doi.org/10.1002/elan.201300126.

[9] J. Du, H. Yang, N. Huang, Y. Dong, Q. Gao, W. Yang, B. Liu, C. Yang, Highly sensitive and selective RNase A recognition systems based on "OFF – ON – OFF" fluorescence probes, Sens. Actuators B Chem. 259 (2018) 282–288. https://doi.org/10.1016/j.snb.2017.12.072.